Inkjet Printing of Biocompatible Luminescent Organic Crystals for Optical Encryption

Ekaterina V Gunina, Irina Gorbunova, Sergey Rzhevskiy, Yuliya Kenzhebayeva, Semyon Bachinin, Daria Shipilovskikh, Kseniya Mitusova, Anna Rogova, Alena N Kulakova, Alexander S Timin, et al.

ACS APPLIED OPTICAL MATERIALS

pubs.acs.org/acsaom Article

Inkjet Printing of Biocompatible Luminescent Organic Crystals for Optical Encryption

Ekaterina V. Gunina, Irina Gorbunova, Sergey Rzhevskiy, Yuliya Kenzhebayeva, Semyon Bachinin, Daria Shipilovskikh, Kseniya Mitusova, Anna Rogova, Alena N. Kulakova, Alexander S. Timin, Sergei Shipilovskikh,* and Valentin A. Milichko*

Cite This: https://doi.org/10.1021/acsaom.3c00340 Read Online

ACCESS | Metrics & More | Article Recommendations | Supporting Information

ABSTRACT: The design and fabrication of optical security marks are of great importance for information encryption and data protection. Herein, biocompatible marks with excellent optical properties, printed easily on arbitrary surfaces, remain a challenge. Here, we report on the design of a series of transparent organic inks based on Gewald's 2-aminothiophene derivatives, which are utilized then for inkjet printing of large-scale invisible images with 60 μm resolution on arbitrary substrates. The encryption regime is provided through a combination of organic inks possessing different photoluminescence (PL) spectra ranging from 584 to 625 nm. The decoding of such images is achieved in the PL regime manually and can be read with the naked eye upon ultraviolet radiation. The high biocompatibility of the inks, confirmed by the epithelial-like cell line of mouse cutaneous melanoma and mouse embryonic fibroblasts, paves the way to scalable inkjet printing of biocompatible images for optical encryption and goods protection.

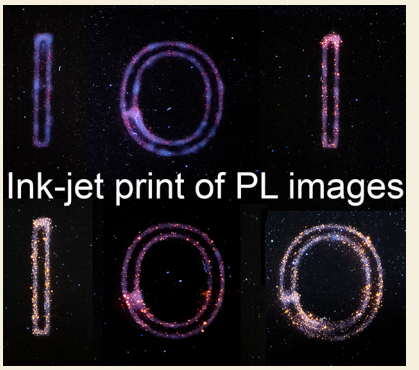

KEYWORDS: *inkjet printing, biocompatible materials, organic crystals, photoluminescence, optical encryption*

1. INTRODUCTION

The rapid growth of the consumer market raises a problem for protecting personal information and goods from counterfeiting, thus forming a new direction in material science and digital technology to encrypt the information.[1−5] One of the promising solutions, combining new materials and encryption technologies, is optical information encryption, since it is a quite fast, remote, safe (including for human health), and low-energy-consumptive approach.[6−16] In most cases, optically active or photoluminescent inorganic, organic, and hybrid materials[17−29] are utilized for optical encryption through a change in their color or photoluminescent (PL) signal. However, the design and fabrication of the optical security marks on arbitrary surfaces with PL decoding, allowing also a human contact, is still in its infancy.

To address this challenge, inkjet printing can be considered a promising method. Indeed, low cost, high efficiency, and precision printing made it the widely used and biocompatible method in industry.[30−33] In its basics, the droplets of inorganic or organics inks are produced with controllable size (up to a single atom) and delivered to a specific location on an arbitrary substrate (solids, flexible polymers, and even skin) to create metallic, dielectric, organic and hybrid patterns, and optical images.[34−44] Besides high efficiency and precision, there are some unique features of inkjet printing such as drop-on-demand, noncontact, and multi-ink delivery. Thereby, the printing is utilized to fabricate planar electronic devices, flexible robots, as well as living cells.[45−50] At the same time, the design of the inks for optical security marks, providing biocompatibility and excellent PL properties for encryption, remains a challenge.

Here, we report on the design of a series of transparent organic inks based on Gewald's 2-aminothiophenes derivatives, which are utilized then for inkjet printing of large-scale invisible images with 60 μm resolution on arbitrary substrates (glass, aluminum, polypropylene, paper, and carton). The encryption regime is provided through a combination of organic inks possessing different PL spectra ranging from 584 to 625 nm. Herein, the decoding of such images is achieved in the PL regime manually and can be read with the naked eye upon ultraviolet radiation. Excellent biocompatibility of the synthesized inks has been confirmed with embryonic fibroblast and cutaneous melanoma cell lines. The cells incubated with the inks at different concentrations retained their viability and morphological features. The results, thereby, pave the way to the scalable inkjet printing of biocompatible images for optical encryption and goods protection.

Received: September 22, 2023
Revised: November 8, 2023
Accepted: November 9, 2023

https://doi.org/10.1021/acsaom.3c00340
ACS Appl. Opt. Mater. XXXX, XXX, XXX−XXX

Scheme 1. Synthesis of Organic Inks (7a–7f).

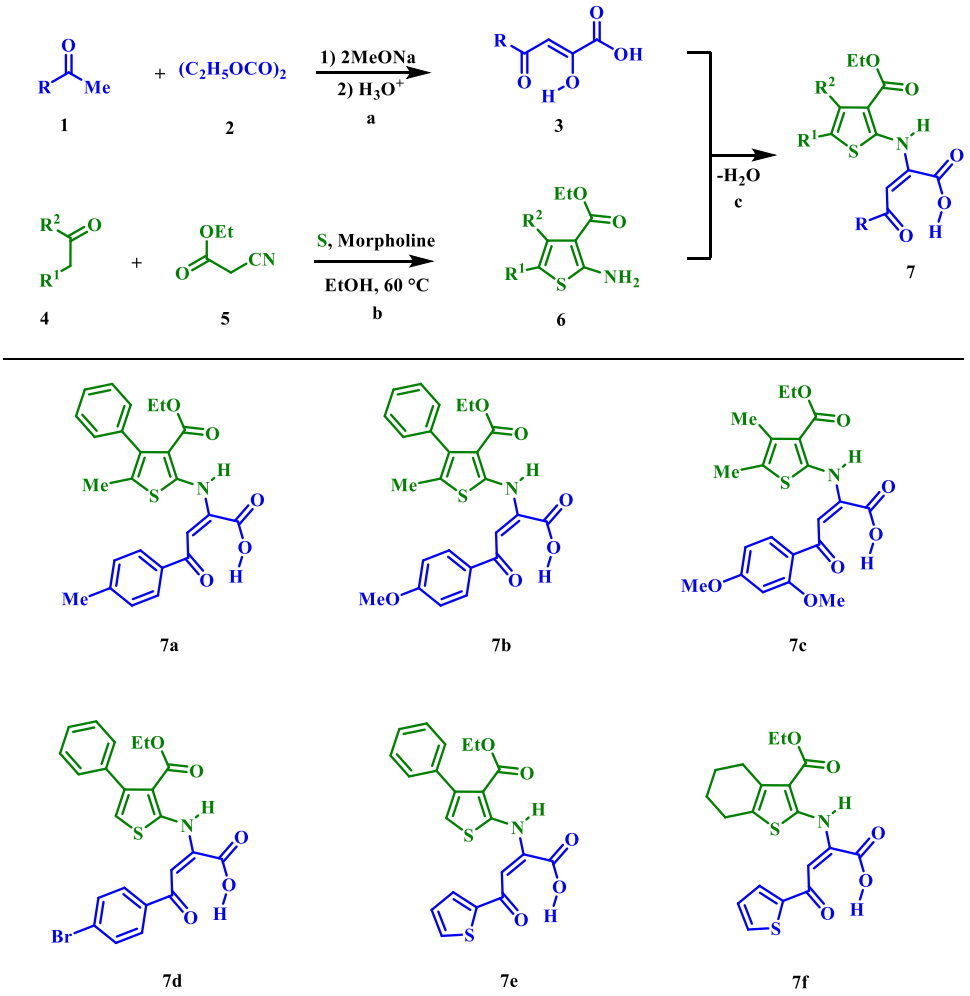

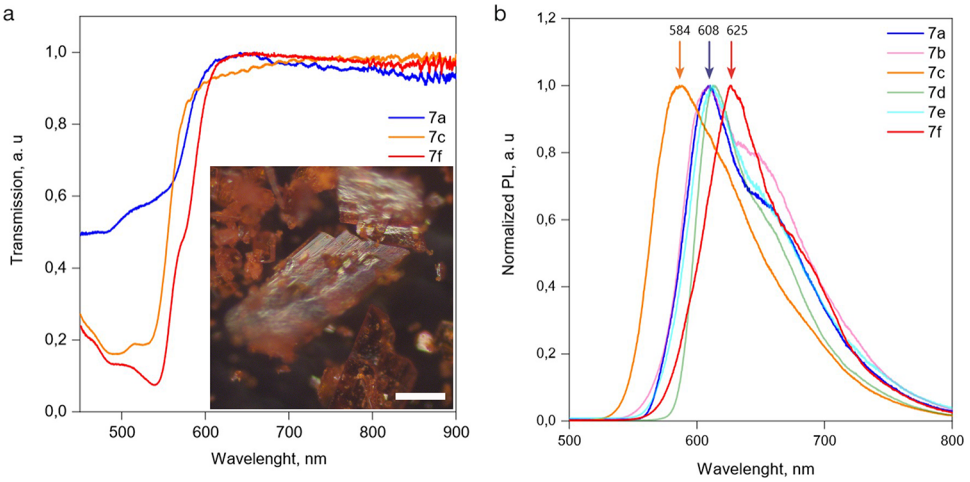

Figure 1. Transmission (a) and PL (b) spectra of **7a–7f** in a dry form (organic crystals). Inset in (a) corresponds to an optical image of the **7f** organic crystal; scale bar, 50 μm. Arrows in (b) indicate the center of PL for **7a** (608 nm), **7c** (584 nm), and **7f** (625 nm).

2. RESULTS AND DISCUSSION

As organic (luminescent) molecules for inks, we have chosen substituted derivatives of Gewald's 2-aminothiophenes. Next to high biocompatibility and a wide range of biological activities,[51,52] these compounds have also been utilized as precursors to design optical materials for solar cells, laser-emitted diodes, and luminescent displays.[53−61] In detail, we have carried out a multistep synthesis of the inks based on substituted 2-amino-4-oxobut-2-enoic acids (**7a–f**), containing Gewald's aminothiophene groups. Preliminarily, the starting intermediates such as substituted 2-hydroxy-4-oxobut-2-enoic acids (**3**) and 2-aminothiophene-3-carboxylic acids (**6**, Scheme 1) have been obtained. On the first step, 2-hydroxy-4-oxobut-

https://doi.org/10.1021/acsaom.3c00340
ACS Appl. Opt. Mater. XXXX, XXX, XXX−XXX

2-enoic acids (**3**) have been synthesized by the Claisen condensation method via the reaction of diethyl oxalate (**2**) with substituted methyl ketones (**1**) in the presence of sodium methoxide (2 equiv) in methanol, with a subsequent decomposition of the intermediate salt (Scheme 1, condition a). Then, the substituted 2-aminothiophene-3-carboxylic acids (**6**) have been prepared by Gewald's reaction of the corresponding substituted ketones (**4**) with ethyl 2-cyanoacetate (**5**) and sulfur in the one-pot method (Scheme 1, condition b). In the final step, the substituted 2-hydroxy-4-oxobut-2-enoic acids (**3**) react with substituted 2-amino-thiophene-3-carboxylic acids (**6**) in ethanol at 60 °C, resulting in the compounds (**7a**−**7f**) based on substituted 2-amino-4-oxobut-2-enoic acid (Scheme 1).

To study the optical properties of the resulting compounds (**7a**−**7f**), we have transferred them to a dry form through solvent (acetonitrile) removal and densification on a glass substrate under normal conditions. The formed organic crystals with an average thickness of 100 μm (Figure 1a, inset) possess a reddish color, which has been confirmed by optical spectroscopy, showing a decrease in transmission at 550 nm (Figure 1a). PL spectroscopy has also been performed for the entire series of the organic compounds (**7a**−**7f**) in a dry form (see sec4). As can be seen in Figure 1b, an optical pumping at 350 nm leads to relatively narrow (90 nm width) PL spectra centered at 584 (for **7c**) to 625 nm (for **7f**). Such 40 nm spectral shift of PL signal with 90 nm width may not be obvious to the naked eye, but it is still sufficient for optical encryption. Therefore, we have selected three types of organic compounds (**7a**, **7c**, and **7f**) which are maximally different from each other in the PL spectra to further create an optically transparent encrypted image for decoding and reading in the ultraviolet PL regime (see below).

At the intermediate stage, we checked the biocompatibility of the selected organic compounds at different concentration ranges. For this, their cytotoxic effect has been evaluated on B16−F10 and MEF MEF2 cells (epithelial-like cell line of mouse cutaneous melanoma and mouse embryonic fibroblasts) using Calcein AM staining. The B16−F10 cell line has been used as a skin model, since it is an epithelial-like cell isolated from skin tissue, while the MEF NF2 cell line has been used as a healthy cell model. The fluorescent images have been obtained using confocal laser scanning microscopy (CLSM, see Figure 2: cells with green fluorescence are living cells). As shown in Figure 2a,b, the CLSM images for **7a**, **7c**, and **7f** clearly demonstrated that the cells are viable, possessing normal morphology at different concentrations (0.125, 0.25, 0.5, and 1 mg mL^{-1}) of each tested compound. In order to quantitatively confirm the nontoxicity of the compounds, IC_{50} values have been calculated using the AlamarBlue analysis. Figure 3a−c shows the cytotoxic efficiency, expressed in IC_{50} values, which represent the concentration of the compounds required to obtain 50% inhibition of cell growth. In detail, Figure 3a represents the histograms of dependence of cell viability on the concentrations of the compounds. Figure 3b shows the calculated curves for IC50 values, while Figure 3c summarizes the IC50 values for **7a**, **7c**, and **7f** in the case of two cell lines (B16−F10 and MEF MEF2). According to the data obtained, all organic compounds possess low toxicity, while **7c** demonstrated the best biocompatibility (IC50 equals to 2.08 mg mL^{-1} in the case of MEF NF2 cells and ∼1.38 mg mL^{-1} for B16−F10 cells).

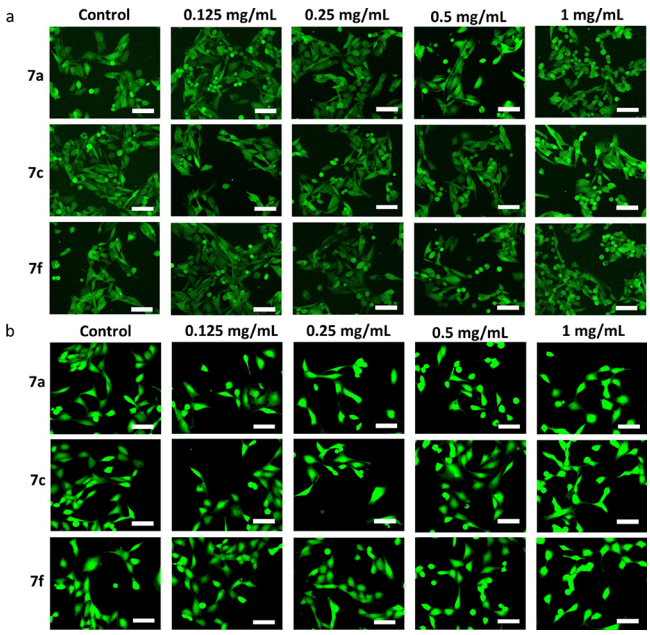

Figure 2. CLSM images of B16−F10 (a) and MEF NF2 (b) cells incubated with the organic compounds (**7a**, **7c**, and **7f**) at different concentrations (0.125−1 mg mL^{-1}) and stained with Calcein AM. Scale bar, 50 μm.

Next, to make organic inks based on the selected compounds for inkjet printing on different substrates (glass, aluminum, polypropylene, paper, and carton), a high-viscosity and wettability solution has been utilized. Since the wetting angle of the substrate corresponds to 90° for water, we have faced with the problem of making a thin image from the water solution of the organic compounds (**7**). To increase the viscosity and wettability of the resulting inks, food gelatin has been used. For this, 1.5 g of gelatin has been dissolved in 150 mL of water under heating and constant stirring, followed by the addition of 0.5 mL of N,N-dimethylformamide for the efficient dissolution of the organic compounds. Then, the selected compounds (**7a**, **7c**, **7f**, and the combination of **7c**−**7f**) have been added to the solution. The solution has been heated to 90 °C with stirring at 1000 rpm and cooled for 24 h at 4 °C to obtain the organic ink. The resulting inks had a viscosity of 1.6 mPa per second (measured on a rotary viscometer), which is higher than that of water (1 mPa per second), while lower than that of gelatin, which has a viscosity ranging from 2 to 10 mPa per second.[62]

Finally, the inkjet printing has been performed on a homemade setup (Figure S2) allowing sequential supply of the inks to create a multicolor planar pattern. An electronically controlled feed of the inks (3 mL drop) through the syringe to a specific place on the substrates has been performed with a 5 mm s^{-1} rate. To vary the brightness of the resulting images (Figure S5), printing was performed several times. After each print, the image has been dried for 1 min at ambient conditions. As one can see in Figures 4 and S3, the printed images are optically transparent (since the thickness is less than 1 μm, the width of the printed lines is about 60 μm; Figure S4) and invisible to the naked eye. However, when an ultraviolet lamp is switched on, the images show their color depending on the PL features. Moreover, the combination of the organic compounds (**7c**−**7f**) gives a shade to the color of

https://doi.org/10.1021/acsaom.3c00340
ACS Appl. Opt. Mater. XXXX, XXX, XXX−XXX

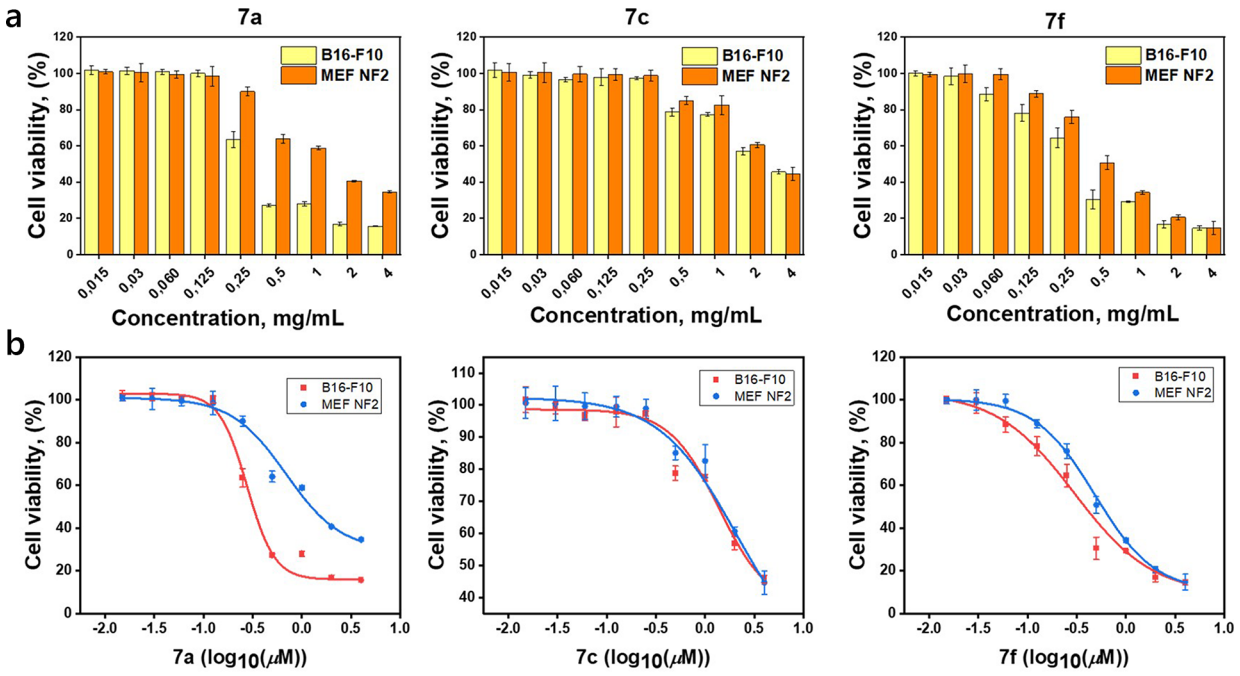

c

Compound	MEF NF2, mg/mL	B16-F10, mg/mL
7a	0.69 ±0.12	0.27 ± 0.038
7c	2.08 ±2.33	1.38 ± 0.30
7f	0.48 ±0.04	0.29 ± 0.035

Figure 3. (a,b) Effect of the organic compounds (**7a**, **7c**, and **7f**) on the viability of B16−F10 and MEF NF2 cells. AlamarBlue assay has been used to assess their cytotoxic activity. Time of incubation was 24 h. The concentration range of the tested compounds was 0.015−4 mg mL^{-1}. (c) IC_{50} values calculated for the tested compounds. The results are shown as average value ± standard deviation (n = 3).

Figure 4. Inkjet-printed images upon ultraviolet irradiation (a) and day light (b). (c−f) PL decoding of the inkjet-printed images based on **7a**, **7f**, and **7c** and a combination of **7c**−**7f** inks.

the resulting images, which can be read as an optically encoded image.

3. CONCLUSIONS

We report on the design of a series of transparent organic inks based on Gewald's 2-aminothiophene derivatives, which are utilized then for inkjet printing of large-scale invisible images with 60 μm resolution on arbitrary substrates (glass, aluminum, polypropylene, paper, and carton). The encryption regime is provided through a combination of organic inks possessing different PL spectra, ranging from 584 to 625 nm. Herein, the decoding of such images is achieved in the PL regime manually and can be read with the naked eye upon ultraviolet radiation. The cytotoxicity assays performed on B16−F10 and MEF NF2 cells confirmed the high biocompatibility of the synthesized inks. The results, thereby, pave the way to scalable inkjet printing of biocompatible images for optical encryption and goods protection.

4. METHODS

4.1. Materials

All of the chemical reagents have been purchased from commercial sources and used without further purification unless otherwise specified. The details are presented in the Supporting Information.

4.2. Synthesis

All the air-sensitive reactions have been carried out under a nitrogen atmosphere in standard Schlenk flasks. All the chemicals were of analytical grade and used without further purification. 4′-Methylacetophenone (95%), 4′-methoxyacetophenone (99%), 2′,4′-dime-

https://doi.org/10.1021/acsaom.3c00340
ACS Appl. Opt. Mater. XXXX, XXX, XXX−XXX

thoxyacetophenone (97%), 4′-bromoacetophenone (98%), 2-acetylthiophene (98%), diethyl oxalate (≥99%), 2-butanone (≥99.0%), acetophenone (99%), propiophenone (99%), cyclohexanone (≥99.0%), sulfur (99.98%), morpholine (≥99%), and ethyl cyanoacetate (≥98%) were purchased from Sigma-Aldrich. Methanol (MeOH), acetonitrile, and ethanol (EtOH) have been dried over activated molecular sieves (3 Å) in Erlenmeyer flasks for 2 days prior to use. Chemically pure grade solvents were subjected to additional purification and drying.

4.3. Characterization

NMR spectra were recorded on Bruker Avance III (400 MHz) and DRX-500 (500 MHz) spectrometers. The chemical shifts (δ) have been measured in parts per million with respect to the solvent (CDCl3, 1δ: δ = 7.26 ppm, 13C: δ = 77.2 ppm; DMSOd6, 1δ: δ = 2.50 ppm, 13C: δ = 39.5 ppm). IR spectra were recorded on an FSM-1202 spectrometer from the samples dispersed in mineral oil. Elemental analysis was performed with a Leco CHNS-932 elemental analyzer. Melting points were determined with Stuart SMP 40. The details are presented in Supporting Information.

4.4. Optical Spectroscopy

A system with two independent optical channels was used to measure the optical transmittance and photoluminescence spectra of single organic crystals.[63−66] Photoluminescence excitation has been carried out by femtosecond laser radiation (Avesta TEMA, 150 fs pulse duration, 1050 nm central wavelength, and 350 nm of third harmonics, and 80 MHz repetition rate), while the optical transmission has been analyzed with the use of a white light lamp (Ocean Optics). Next, the laser radiation passed through the bottom optical channel with an objective (50×, 0.46 NA). The re-emitted or transmitted optical signal has been collected by the top optical channel (objective 50×, 0.46 NA) and then analyzed via a HORIBA LabRam confocal spectrometer with a water-cooling charge-coupled device (CCD, Andor DU 420A-OE 325) with 150 g mm^{-1} diffraction grating.

All photoluminescent images printed on glass, aluminum, polypropylene, paper, and carton in Figures 4 and S3 have been obtained in the reflection mode when UV pumping illuminated the image from the observer's side.

4.5. Cell Viability Analysis

For in vitro studies, an epithelial-like cell line of mouse cutaneous melanoma B16−F10 cultured in αMEM (Alpha Modification of Eagle's Medium) with the addition of 10% FBS (fetal bovine serum) has been used. A line of mouse embryonic fibroblasts MEF NF2 cultured in DMEM (Dulbecco's modified Eagle's medium) with the addition of 10% FBS has been used as a normal cell line. Then, cells were incubated in a humidified atmosphere, containing 5% CO2 at 37 °C.

Calcein AM staining was used to observe cell morphology and their survival. AlamarBlue assays have been used to study the viability of cells after their incubation with organic compounds at various concentrations. The detailed protocols for these experiments are provided in the Supporting Information. The Calcein AM staining was performed using inks at concentrations of 0.125, 0.25, 0.5, and 1 mg mL^{-1} after 24 h of incubation. The cells have been then visualized using a confocal laser scanning microscope (CLSM, SP8 Leica).

For the AlamarBlue assay, B16−F10 and MEF NF2 cells were seeded into a 96-well plate (10^4 cells per 100 μL) and incubated overnight at 5% CO2, 37 °C. Before addition to cell cultures, all tested compounds were dissolved in 10 μL of DMSO and then diluted in a cellular medium (4 mg mL^{-1}). After that, several concentrations of the tested compounds were added (0.015, 0.03, 0.06, 0.125, 0.25, 0.5, 1, 2, and 4 mg mL^{-1}) into the wells with cells (B16−F10 and MEF NF2) and incubated for 24 h. After that, the cell medium was removed, and AlamarBlue (10% by w/w) was added to each well. All wells were incubated for 4 h at 5% CO_2 and 37 °C and rechecked for color change. The absorption was analyzed on a spectrophotometric microplate reader at wavelengths of 570 and 600 nm. Untreated cells were used as control cells. The results were evaluated according to the formula given in the Supporting Information.

4.6. Inkjet Printing

The "drop-on-demand" inkjet technology has been used to build the setup (Figure S2) containing a 3D manipulator and a controller with a modified open Marlin firmware. A syringe pump was installed as an extruder (the element that feeds the material during the inkjet printing). The volume of the ink drops can be varied, and we set a value of 3 mL. The needle of the printing syringe has been sharpened in a special way, so that, on the one hand, it was parallel to the substrate and, on the other, not to scratch it when printing, even with small distortions. Based on a 3D model, the image has been generated in special software for installing the inkjet printing, taking into account the process parameters, selected during the experiments. The optimal printing rate was 5 mm/s, while the line thickness was 0.01 mm.

■ ASSOCIATED CONTENT

Supporting Information

The Supporting Information is available free of charge at https://pubs.acs.org/doi/10.1021/acsaom.3c00340.

Synthesis, NMR, biocompatibility experiments, SEM, and images on arbitrary substrates (PDF)

■ AUTHOR INFORMATION

Corresponding Authors

Sergei Shipilovskikh − *School of Physics and Engineering, ITMO University, St. Petersburg 197101, Russia; Perm State University, Perm 614990, Russia*; Email: s.shipilovskikh@metalab.ifmo.ru

Valentin A. Milichko − *School of Physics and Engineering, ITMO University, St. Petersburg 197101, Russia; Institut Jean Lamour, Université de Lorraine, 54011 Nancy, France*; orcid.org/0000-0002-8461-0804; Email: v.milichko@metalab.ifmo.ru

Authors

Ekaterina V. Gunina − *School of Physics and Engineering, ITMO University, St. Petersburg 197101, Russia*; orcid.org/0000-0002-1422-5599

Irina Gorbunova − *School of Physics and Engineering, ITMO University, St. Petersburg 197101, Russia; Perm State University, Perm 614990, Russia*

Sergey Rzhevskiy − *School of Physics and Engineering, ITMO University, St. Petersburg 197101, Russia*

Yuliya Kenzhebayeva − *School of Physics and Engineering, ITMO University, St. Petersburg 197101, Russia*

Semyon Bachinin − *School of Physics and Engineering, ITMO University, St. Petersburg 197101, Russia*

Daria Shipilovskikh − *Perm National Research Polytechnic University, Perm 614990, Russia*; orcid.org/0000-0001-6086-4300

Kseniya Mitusova − *Peter The Great St. Petersburg Polytechnic University, St. Petersburg 195251, Russia*

Anna Rogova − *Peter The Great St. Petersburg Polytechnic University, St. Petersburg 195251, Russia*

Alena N. Kulakova − *School of Physics and Engineering, ITMO University, St. Petersburg 197101, Russia*

Alexander S. Timin − *Peter The Great St. Petersburg Polytechnic University, St. Petersburg 195251, Russia*; orcid.org/0000-0002-0276-7892

Complete contact information is available at:

https://doi.org/10.1021/acsaom.3c00340
ACS Appl. Opt. Mater. XXXX, XXX, XXX−XXX

https://pubs.acs.org/10.1021/acsaom.3c00340

Notes

The authors declare no competing financial interest.

■ ACKNOWLEDGMENTS

V.A.M. acknowledges the financial support from the Russian Science Foundation (optical part, grant no. 22-72-10027 "Flexible hybrid materials as active layer in memory devices") and the Priority 2030 Federal Academic Leadership Program. S.A.S. acknowledges the financial support by the Government of the Russian Federation through the ITMO Fellowship and Professorship Program and the Russian Science Foundation (chemical part, grant no. 22-73-10069 "Design and application of flexible metal organic frameworks for photonics devices"). A.N.K. acknowledges the financial support by the Government of the Russian Federation through the ITMO Fellowship and Professorship Program and the Russian Science Foundation (SEM analysis, grant no. 23-73-01235). A.S.T. acknowledges the Ministry of Science and Higher Education of Russian Federation FSEG-2022-0012 (in vivo studies with cells).

■ REFERENCES

(1) Froelicher, D.; Troncoso-Pastoriza, J. R.; Raisaro, J. L.; Cuendet, M. A.; Sa Sousa, J.; Cho, H.; Berger, B.; Fellay, J.; Hubaux, J.-P. Truly Privacy-Preserving Federated Analytics for Precision Medicine with Multiparty Homomorphic Encryption. *Nat. Commun.* **2021**, *12*, 5910.

(2) Wu, C.; Wu, F.; Lyu, L.; Qi, T.; Huang, Y.; Xie, X. A Federated Graph Neural Network Framework for Privacy-Preserving Personalization. *Nat. Commun.* **2022**, *13*, 3091.

(3) Wan, Z.; Hazel, J. W.; Clayton, E. W.; Vorobeychik, Y.; Kantarcioglu, M.; Malin, B. A. Sociotechnical Safeguards for Genomic Data Privacy. *Nat. Rev. Genetics* **2022**, *23*, 429−445.

(4) Fisher, K. A. G.; Broadbent, A.; Shalm, L. K.; Yan, Z.; Lavoie, J.; Prevedel, R.; Jennewein, T.; Resch, K. J. Quantum Computing on Encrypted Data. *Nat. Commun.* **2014**, *5*, 3074.

(5) Şatir, E.; Kendirli, O. A Symmetric DNA Encryption Process with a Biotechnical Hardware. *J. King Saud Univ. Sci.* **2022**, *34*, No. 101838.

(6) Bai, B.; Wei, H.; Yang, X.; Gan, T.; Mengu, D.; Jarrahi, M.; Ozcan, A. Data-Class-Specific All-Optical Transformations and Encryption. *Adv. Mater.* **2023**, *35*, No. 2212091.

(7) Liu, S.; Guo, C.; Sheridan, J. T. A Review of Optical Image Encryption Techniques. *Opt. Laser Technol.* **2014**, *57*, 327−342.

(8) Hazer, A.; Yıldırım, R. A. Review of Single and Multiple Optical Image Encryption Techniques. *J. Opt.* **2021**, *23*, 113501.

(9) Qu, G.; Yang, W.; Song, Q.; Liu, Y.; Qiu, C. W.; Han, J.; Tsai, D. P.; Xiao, S. Reprogrammable Meta-Hologram for Optical Encryption. *Nat. Commun.* **2020**, *11*, 5484.

(10) Ouyang, M.; Yu, H.; Pan, D.; Wan, L.; Zhang, C.; Gao, S.; Feng, T.; Li, Z. Optical Encryption in Spatial Frequencies of Light Fields with Metasurfaces. *Optica* **2022**, *9*, 1022−1028.

(11) Chen, L.; Gan, W.; Chen, L.; Mao, H. Optical Encryption Technology based on Spiral Phase Coherent Superposition and Vector Beam Generation System. *Optik* **2022**, *253*, No. 168599.

(12) Mosso, E. An Optical-Cryptographic Encryption Scheme using a Keystream Synthesizer based on Chaotic Speckle Nature. *J. Opt.* **2023**, *25*, No. 015703.

(13) Optical Encryption and Decryption. In *Generalized Phase Contrast. Springer Series in Optical Sciences*; Springer: Dordrecht, 2009; pp 273-298.

(14) Naughton, T. J.; Hennelly, B. M.; Dowling, T. Introducing Secure Modes of Operation for Optical Encryption. *J. Opt. Soc. Am. A* **2008**, *25*, 2608−2617.

(15) He, M.; Tan, Q.; Cao, L.; He, Q.; Jin, G. Security Enhanced Optical Encryption System by Random Phase Key and Permutation Key. *Opt. Express* **2009**, *17*, 22462−22473.

(16) Moon, J.; Cho, Y.-C.; Kang, S.; Jang, M.; Choi, W. Measuring the Scattering Tensor of a Disordered Nonlinear Medium. *Nature Phys.* **2023**, *19*, 1709.

(17) Larin, A. O.; Dvoretckaia, L. N.; Mozharov, A. M.; Mukhin, I. S.; Cherepakhin, A. B.; Shishkin, I. I.; Ageev, E. I.; Zuev, D. A. Luminescent Erbium-Doped Silicon Thin Films for Advanced Anti-Counterfeit Labels. *Adv. Mater.* **2021**, *33*, No. 2005886.

(18) Syubaev, S.; Gordeev, I.; Modin, E.; Terentyev, V.; Storozhenko, D.; Starikov, S.; Kuchmizhak, A. A. Security Labeling and Optical Information Encryption Enabled by Laser-Printed Silicon Mie Resonators. *Nanoscale* **2022**, *14*, 16618−16626.

(19) Liu, S.; Wang, X.; Ni, J.; Cao, Y.; Li, J.; Wang, C.; Hu, Y.; Chu, J.; Wu, D. Optical Encryption in the Photonic Orbital Angular Momentum Dimension via Direct-Laser-Writing 3D Chiral Metahelices. *Nano Lett.* **2023**, *23*, 2304−2311.

(20) Bozzio, M.; Vyvlecka, M.; Cosacchi, M.; Nawrath, C.; Seidelmann, T.; Loredo, J. C.; Portalupi, S. L.; Axt, V. M.; Michler, P.; Walther, P. Enhancing Quantum Cryptography with Quantum Dot Single-Photon Sources. *npj Quantum Inform.* **2022**, *8*, 104.

(21) Wang, Q.; Lin, B.; Chen, M.; Zhao, C.; Tian, H.; Qu, D. H. A Dynamic Assembly-Induced Emissive System for Advanced Information Encryption with Time-Dependent Security. *Nat. Commun.* **2022**, *13*, 4185.

(22) Wang, C.; Zhang, D.; Yue, J.; Zhang, X.; Lin, H.; Sun, X.; Cui, A.; Zhang, T.; Chen, C.; Fei, T. Dual-Layer Optical Encryption Fluorescent Polymer Waveguide Chip based on Optical Pulse-Code Modulation Technique. *Nat. Commun.* **2023**, *14*, 4578.

(23) Wu, T.; Ma, J.; Wang, C.; Wang, H.; Cao, L.; Su, P. Optical Encryption Based on Computer Generated Holograms in Photopolymer. *Polymers* **2021**, *13*, 1358.

(24) Hu, Y.; Huang, Z.; Willner, I.; Ma, X. Multicolor Circularly Polarized Luminescence of a Single-Component System Revealing Multiple Information Encryption. *CCS Chem.* **2023**, 1.

(25) Zhang, C.; Wang, B.; Li, W.; Huang, S.; Kong, L.; Li, Z.; Li, L. Conversion of Invisible Metal-Organic Frameworks to Luminescent Perovskite Nanocrystals for Confidential Information Encryption and Decryption. *Nat. Commun.* **2017**, *8*, 1138.

(26) Yu, J.; Han, Y.; Wang, L.; Liu, Y.; Zhang, H.; Chen, X.; Liu, X.; Wang, Z.; Hu, J. Metal−Organic Framework-Based Ultrafast Logic Gates for High-Security Optical Encryption. *Ultrafast Sci.* **2023**, *3*, No. 0030.

(27) Liu, Y.; Zhang, Y. Moving Binary-Color Heterojunction for Spatiotemporal Multilevel Encryption via Directional Swelling and Anion Exchange. *ACS Nano* **2021**, *15*, 7628−7637.

(28) Milichko, V. A.; Makarov, S. V.; Yulin, A. V.; Vinogradov, A. V.; Krasilin, A. A.; Ushakova, E.; Dzyuba, V. P.; Hey-Hawkins, E.; Pidko, E. A.; Belov, P. A. van der Waals Metal-Organic Framework as an Excitonic Material for Advanced Photonics. *Adv. Mater.* **2017**, *29*, No. 1606034.

(29) Kulachenkov, N.; Barsukova, M.; Alekseevskiy, P.; Sapianik, A. A.; Sergeev, M.; Yankin, A.; Krasilin, A. A.; Bachinin, S.; Shipilovskikh, S.; Poturaev, P.; Medvedeva, N.; Denislamova, E.; Zelenovskiy, P. S.; Shilovskikh, V. V.; Kenzhebayeva, Y.; Efimova, A.; Novikov, A. S.; Lunev, A.; Fedin, V. P.; Milichko, V. A. Dimensionality Mediated Highly Repeatable and Fast Transformation of Coordination Polymer Single Crystals for All-Optical Data Processing. *Nano Lett.* **2022**, *22* (17), 6972−6981.

(30) *Inkjet Printing in Industry: Materials, Technologies, Systems, and Applications*; Zapka, W., Ed.; Wiley VCH GmbH, 2022.

(31) Li, X.; Liu, B.; Pei, B.; Chen, J.; Zhou, D.; Peng, J.; Zhang, X.; Jia, W.; Xu, T. Inkjet Bioprinting of Biomaterials. *Chem. Rev.* **2020**, *120*, 10793−10833.

(32) Jeong, H. Y.; Lee, E.; An, S. C.; Lim, Y.; Ju, Y. C. 3D and 4D Printing for Pptics and Metaphotonics. *Nanophotonics* **2020**, *9*, 1139−1160.

(33) Mani, M. P.; Sadia, M.; Jaganathan, S. K.; Khudzari, A. Z.; Supriyanto, E.; Saidin, S.; Ramakrishna, S.; Ismail, A. F.; Faudzi, A. A. M. A Review on 3D Printing in Tissue Engineering Applications. *J. Polym. Eng.* **2022**, *42*, 243−265.
(34) Zhang, Y.; Zhang, F.; Yan, Z.; Ma, Q.; Li, X.; Huang, Y.; Rogers, J. A. Printing, Folding and Assembly Methods for Forming 3D Mesostructures in Advanced Materials. *Nat. Rev. Mater.* **2017**, *2*, 17019.
(35) Jung, W.; Jung, Y. H.; Pikhitsa, P. V.; Feng, J.; Yang, Y.; Kim, M.; Tsai, H. Y.; Tanaka, T.; Shin, J.; Kim, K. Y.; Choi, H.; Rho, J.; Choi, M. Three-Dimensional Nanoprinting via Charged Aerosol Jets. *Nature* **2021**, *592*, 54−59.
(36) Wen, X.; Zhang, B.; Wang, W.; Ye, F.; Yue, S.; Guo, H.; Gao, G.; Zhao, Y.; Fang, Q.; Nguyen, C.; Zhang, X.; Bao, J.; Robinson, J. T.; Ajayan, P. M.; Lou, J. 3D-Printed Silica with Nanoscale Resolution. *Nat. Mater.* **2021**, *20*, 1506−1511.
(37) Walker, D. A.; Hedrick, J. L.; Mirkin, C. A. Rapid, Large-Volume, Thermally Controlled 3D Printing using a Mobile Liquid Interface. *Science* **2019**, *366*, 360−364.
(38) Tumbleston, J. R.; Shirvanyants, D.; Ermoshkin, N.; Janusziewicz, R.; Johnson, A. R.; Kelly, D.; Chen, K.; Pinschmidt, R.; Rolland, J. P.; Ermoshkin, A.; Samulski, E. T.; DeSimone, J. M. Continuous Liquid Interface Production of 3D Objects. *Science* **2015**, *347*, 1349−1352.
(39) Li, W.; Wang, Y.; Li, M.; Garbarini, L. P.; Omenetto, F. G. Inkjet Printing of Patterned, Multispectral, and Biocompatible Photonic Crystals. *Adv. Mater.* **2019**, *31*, No. 1901036.
(40) McManus, D.; Vranic, S.; Withers, F.; Sanchez-Romaguera, V.; Macucci, M.; Yang, H.; Sorrentino, R.; Parvez, K.; Son, S. K.; Iannaccone, G.; Kostarelos, K.; Fiori, G.; Casiraghi, C. Water-based and Biocompatible 2D Crystal Inks for All-Inkjet-Printed Heterostructures. *Nature Nanothechnol.* **2017**, *12*, 343−350.
(41) Hossain, R. F.; Deaguero, I. G.; Boland, T.; Kaul, A. B. Biocompatible, Large-Format, Inkjet Printed Heterostructure MoS2-Graphene Photodetectors on Conformable Substrates. *npj 2D Mater. App.* **2017**, *1*, 28.
(42) Hart, L. R.; Li, S.; Sturgess, C.; Wildman, R.; Jones, J. R.; Hayes, W. 3D Printing of Biocompatible Supramolecular Polymers and their Composites. *ACS Appl. Mater. Interfaces* **2016**, *8*, 3115−3122.
(43) Zheng, X.; Zhu, Y.; Liu, Y.; Zhou, L.; Xu, Z.; Feng, C.; Zheng, C.; Zheng, Y.; Bai, J.; Yang, K.; Zhu, D.; Yao, J.; Hu, H.; Zheng, Y.; Guo, T.; Li, F. Inkjet-Printed Quantum Dot Fluorescent Security Labels with Triple-Level Optical Encryption. *ACS Appl. Mater. Interfaces* **2021**, *13*, 15701−15708.
(44) Yakovlev, A. V.; Milichko, V. A.; Vinogradov, V. V.; Vinogradov, A. V. Inkjet Color Printing by Interference Nanostructures. *ACS Nano* **2016**, *10*, 3078−3086.
(45) Abele, T.; Messer, T.; Jahnke, K.; Hippler, M.; Bastmeyer, M.; Wegener, M.; Göpfric, K. Two-Photon 3D Laser Printing Inside Synthetic Cells. *Adv. Mater.* **2022**, *34*, No. 2106709.
(46) Daly, A. C.; Davidson, M. D.; Burdick, J. A. 3D Bioprinting of High Cell-Density Heterogeneous Tissue Models Through Spheroid Fusion Within Self-Healing Hydrogels. *Nat. Commun.* **2021**, *12*, 753.
(47) Negro, A.; Cherbuin, T.; Lutolf, M. P. 3D Inkjet Printing of Complex. *Cell-Laden Hydrogel Structures. Sci. Rep.* **2018**, *8*, 17099.
(48) Park, J. A.; Yoon, S.; Kwon, J.; Now, H.; Kim, Y. K.; Kim, W. J.; Yoo, J. Y.; Jung, S. Freeform Micropatterning of Living Cells into Cell Culture Medium using Direct Inkjet Printing. *Sci. Rep.* **2018**, *7*, 14610.
(49) Derby, B. Bioprinting: Inkjet Printing Proteins and Hybrid Cell-Containing Materials and Structures. *J. Mater. Chem.* **2008**, *18*, 5717−5721.
(50) Xu, T.; Jin, J.; Gregory, C.; Hickman, J. J.; Boland, T. Inkjet Printing of Viable Mammalian Cells. *Biomaterials* **2005**, *26*, 93−99.
(51) Rogova, A.; Gorbunova, I. A.; Karpov, T. E.; Sidorov, R. Y.; Rubtsov, A. E.; Shipilovskikh, D. A.; Muslimov, A. R.; Zyuzin, M. V.; Timin, A. S.; Shipilovskikh, S. A. Synthesis of Thieno[3,2-e]pyrrolo-[1,2-a]pyrimidine Derivatives and Their Precursors Containing 2-Aminothiophenes Fragments as Anticancer Agents for Therapy of Pulmonary Metastatic Melanoma. *Eur. J. Med. Chem.* **2023**, *254*, No. 115325.
(52) Wang, W.; He, J.; Yang, J.; Zhang, C.; Cheng, Z.; Zhang, Y.; Zhang, Q.; Wang, P.; Tang, S.; Wang, X.; Liu, M.; Lu, W.; Zhang, H. K. Scaffold Hopping Strategy to Identify Prostanoid EP4 Receptor Antagonists for Cancer Immunotherapy. *J. Med. Chem.* **2022**, *65*, 7896−7917.
(53) Small, C. E.; Chen, S.; Subbiah, J.; Amb, C. M.; Tsang, S. W.; Lai, T. H.; Reynolds, J. R.; So, F. High-Efficiency Inverted Dithienogermole−Thienopyrrolodione-based Polymer Solar Cells. *Nature Photon.* **2012**, *6*, 115−120.
(54) Amb, C. M.; Chen, S.; Graham, K. R.; Subbiah, J.; Small, C. E.; So, F.; Reynolds, J. R. Dithienogermole As a Fused Electron Donor in Bulk Heterojunction Solar Cells. *J. Am. Chem. Soc.* **2011**, *133*, 10062−10065.
(55) Bohra, H.; Wang, M. Direct C−H Arylation: a "Greener" Approach Towards Facile Synthesis of Organic Semiconducting Molecules and Polymers. *J. Mater. Chem. A* **2017**, *5*, 11550−11571.
(56) Robitaille, A.; Perea, A.; Bélanger, D.; Leclerc, M. Poly(5-alkylthieno[3,4-c]pyrrole-4,6-dione): A Study of π-Conjugated Redox Polymers as Anode Materials in Lithium-Ion Batteries. *J. Mater. Chem. A* **2017**, *5*, 18088−18094.
(57) Gunina, E.; Timofeeva, M.; Kenzhebayeva, Y. A.; Bachinin, S.; Gorbunova, I. A.; Shipilovskikh, D. A.; Milichko, V. A.; Shipilovskikh, S. A. Thiophene-based Thin Films with Tunable Red Photoluminescence. *Photon. Nanostruct. Fund. App.* **2023**, *56*, No. 101168.
(58) Çakal, D.; Ertan, S.; Cihaner, A.; Önal, A. M. Synthesis and Electrochemical Polymerization of D-A-D Type Monomers with Thieno[3,4-c]pyrrole-4,6-dione Acceptor Unit. *Dyes Pigm.* **2018**, *158*, 175−182.
(59) Gunina, E.; Zhestkij, N.; Bachinin, S.; Fisenko, S. P.; Shipilovskikh, D. A.; Milichko, V. A.; Shipilovskikh, S. A. The Influence of Substitutes on the Room Temperature Photoluminescence of 2-Amino-4-Oxobut-2-Enoic Acid Molecular Crystals. *Photon. Nanostruct. Fund. App.* **2022**, *48*, No. 100990.
(60) Berrouard, P.; Dufresne, S.; Pron, A.; Veilleux, J.; Leclerc, M. Low-Cost Synthesis and Physical Characterization of Thieno[3,4-c]pyrrole-4,6-dione-Based Polymers. *J. Org. Chem.* **2012**, *77* (18), 8167−8173.
(61) Brandner, L.; Müller, T. J. J. Multicomponent Synthesis of Chromophores − The One-Pot Approach to Functional π-Systems. *Front. Chem.* **2023**, *11*, No. 1124209.
(62) Yunoki, S.; Sugimoto, K.; Ohyabu, Y.; Ida, H.; Hiraoka, Y. Accurate and Precise Viscosity Measurements of Gelatin Solutions Using a Rotational Rheometer. *Food Sci. Technol. Res.* **2019**, *25*, 217−226.
(63) Kulachenkov, N. K.; Sun, D.; Mezenov, Y. A.; Yankin, A. N.; Rzhevskiy, S.; Dyachuk, V.; Nominé, A.; Medjahdi, G.; Pidko, E. A.; Milichko, V. A. Photochromic Free MOF-Based Near-Infrared Optical Switch. *Angew. Chemie Int. Ed.* **2020**, *59*, 15522−15526.
(64) Vinogradov, A. V.; Milichko, V. A.; Zaake-Hertling, H.; Aleksovska, A.; Gruschinski, S.; Schmorl, S.; Kersting, B.; Zolnhofer, E. M.; Sutter, J.; Meyer, K.; Lönnecke, P.; Hey-Hawkins, E. Unique Anisotropic Optical Properties of a Highly Stable Metal−Organic Framework based on Trinuclear Iron(III) Secondary Building units Linked by Tetracarboxylic Linkers with an Anthracene Core. *Dalton Trans.* **2016**, *45*, 7244−7249.
(65) Kulachenkov, N. K.; Bruyere, S.; Sapchenko, S. A.; Mezenov, Y. A.; Sun, D.; Krasilin, A. A.; Nominé, A.; Ghanbaja, J.; Belmonte, T.; Fedin, V. P.; Pidko, E. A.; Milichko, V. A. Ultrafast Melting of Metal−Organic Frameworks for Advanced Nanophotonics. *Adv. Funct. Mater.* **2020**, *30*, No. 1908292.
(66) Vinogradov, V. V.; Drozdov, A. S.; Mingabudinova, L. R.; Shabanova, E. M.; Kolchina, N. O.; Anastasova, E. I.; Markova, A. A.; Shtil, A. A.; Milichko, V. A.; Starova, G. L.; Precker, R. L. M.; Vinogradov, A. V.; Hey-Hawkins, E.; Pidko, E. A. Composites based on Heparin and MIL-101(Fe): the Drug Releasing Depot for Anticoagulant Therapy and Advanced Medical Nanofabrication. *J. Mater. Chem. B* **2018**, *6*, 2450−2459.

https://doi.org/10.1021/acsaom.3c00340
ACS Appl. Opt. Mater. XXXX, XXX, XXX−XXX